

# POSITRON PRODUCTION BY LASER LIGHT

Kirk T. McDonald\*  
Joseph Henry Laboratories  
Princeton University, Princeton, NJ 08544

REPRESENTING THE E-144 COLLABORATION<sup>†‡</sup>

## ABSTRACT

A signal of  $106 \pm 14$  positrons above background has been observed in collisions of a low-emittance 46.6-GeV electron beam with terawatt pulses from a Nd:glass laser at 527 nm wavelengths in an experiment at the Final Focus Test Beam at SLAC. The positrons are interpreted as arising from a two-step process in which laser photons are backscattered to GeV energies by the electron beam, followed by a collision between the high-energy photon and several laser photons to produce an electron-positron pair. These results are the first laboratory evidence for inelastic light-by-light scattering involving only real photons.

---

\*Supported by DOE Grant DE-FG02-91ER40671.

<sup>†</sup>See Acknowledgments.

<sup>‡</sup>© 1997 by Kirk T. McDonald.

# 1 Introduction

This paper discusses recent experimental results obtained by the E-144 Collaboration on the interactions of electrons and photons in very intense electromagnetic fields.<sup>1-4</sup>

## 1.1 Hawking-Unruh Radiation

My own interest in this field was sparked in the early 1980s by conversations with then Princeton graduate student Nathan Myhrvold<sup>5</sup> regarding Hawking radiation.<sup>6</sup> According to Hawking, an observer outside a black hole experiences a bath of thermal radiation of temperature

$$T = \frac{\hbar g}{2\pi ck}, \quad (1)$$

where  $g$  is the local acceleration due to gravity,  $c$  is the speed of light,  $\hbar$  is Planck's constant, and  $k$  is Boltzmann's constant. In some manner the background gravitational field interacts with the quantum fluctuations of the electromagnetic field, with the result that energy can be transferred to the observer as if he/she were in an oven filled with black-body radiation. Of course, the effect is strong only if the background field is strong.

An extreme example is that if the temperature is equivalent to 1 MeV or more, virtual electron-positron pairs emerge from the vacuum into real particles.

As remarked by Unruh,<sup>7</sup> this phenomenon can be demonstrated in the laboratory according to the principle of equivalence: An accelerated observer in a gravity-free environment experiences the same physics (locally) as an observer at rest in a gravitational field. Therefore, an accelerated observer (in zero gravity) should find himself/herself in a thermal bath of radiation characterized by temperature

$$T = \frac{\hbar a^*}{2\pi ck}, \quad (2)$$

where  $a^*$  is the acceleration as measured in the observer's instantaneous rest frame.\*

---

\*The Hawking-Unruh temperature finds application in accelerator physics as the reason that electrons in a storage ring do not reach 100% polarization despite emitting polarized synchrotron radiation.<sup>8</sup> Indeed, the limiting features of performance of a storage ring that arise due to quantum fluctuations of the synchrotron radiation can be understood quickly in terms of Eq. (2) (Ref. 9).

Suppose the observer is an electron accelerated by an electromagnetic field  $E$ , and that the characteristic energy  $kT$  from Eq. (2) is much less than 1 MeV. Then, Thomson scattering of the electron off photons in the apparent thermal bath would be interpreted by a laboratory observer as an extra contribution to the radiation rate of the accelerated charge.<sup>10,11</sup> The power of the extra radiation, which I call Unruh radiation, is given by

$$\frac{dU_{\text{Unruh}}}{dt} = (\text{energy flux of thermal radiation}) \times (\text{scattering cross section}). \quad (3)$$

For the scattering cross section we take  $\sigma_{\text{Thomson}} = 8\pi r_0^2/3$ , where  $r_0 = e^2/mc^2$  is the classical electron radius. The energy density of thermal radiation is given by the usual Planck expression:

$$\frac{dU}{d\nu} = \frac{8\pi}{c^3} \frac{h\nu^3}{e^{h\nu/kT} - 1}, \quad (4)$$

where  $\nu$  is the frequency. The flux of the isotropic radiation on the electron is just  $c$  times the energy density. Note that these relations hold in the instantaneous rest frame of the electron. Then,

$$\frac{dU_{\text{Unruh}}}{dt d\nu} = \frac{8\pi}{c^2} \frac{h\nu^3}{e^{h\nu/kT} - 1} \frac{8\pi}{3} r_0^2. \quad (5)$$

On integrating over  $\nu$  we find

$$\frac{dU_{\text{Unruh}}}{dt} = \frac{8\pi^3 \hbar r_0^2}{45c^2} \left( \frac{kT}{\hbar} \right)^4 = \frac{\hbar r_0^2 a^{*4}}{90\pi c^6}, \quad (6)$$

using the Hawking-Unruh relation (2).

This equals the Larmor radiation rate,  $dU/dt = 2e^2 a^{*2}/3c^3$ , when the acceleration  $a^* = eE^*/m$  is about  $10^{30} g$ , *i.e.*, when

$$E^* = \sqrt{\frac{15}{\alpha}} \frac{m^2 c^3}{e\hbar} \approx 6 \times 10^{17} \text{ V/cm}, \quad (7)$$

where  $\alpha = e^2/4\pi\hbar c$  is the fine-structure constant.

## 1.2 The QED Critical Field

The electric field needed for Unruh radiation to become large relative to Larmor radiation is very large! Indeed, it is larger than the so-called QED critical field strength

$$E_{\text{crit}} = \frac{m^2 c^3}{e\hbar} = \frac{mc^2}{e\lambda_C} = 1.3 \times 10^{16} \text{ V/cm} = 4.3 \times 10^{13} \text{ Gauss}, \quad (8)$$

where  $\lambda_C = \hbar/mc$  is the Compton wavelength of the electron. At this field the vacuum is unstable against spontaneous creation of electron-positron pairs.<sup>†</sup>

Thus, before one can study Unruh radiation, physics near the QED critical field strength must be explored. Such fields are not common in nature, but are thought to occur at the surface of neutron stars,<sup>16</sup> and may play a role in pulsar physics.

Critical fields can be temporarily created in the laboratory by the superposition of Coulomb fields during the collision of two heavy nuclei. Indeed, positrons have been observed to emerge from such collisions, but with some controversy as to their interpretation.<sup>17</sup>

The approach of our experiment to critical fields was presaged by Pomeranchuk,<sup>18</sup> who noted that the Earth's magnetic field is critical according to a cosmic-ray electron of energy  $10^{19}$  eV, taking into account the relativistic transformation of fields.

A 50-GeV electron at SLAC has a Lorentz factor  $\gamma \approx 10^5$ . If the electron collides head-on with a laser beam of field strength  $E$ , then the field strength in the rest frame of the electron is  $E^* = 2\gamma E$ . Hence, if the laboratory field strength of the focused laser beam is  $E = 6.5 \times 10^{10}$  V/cm, the field appears to be critical from the point of view of the electron. The corresponding laser intensity is

$$I = \frac{(E[\text{V/cm}])^2}{377\Omega} = 1.1 \times 10^{19} [\text{Watt/cm}^2]. \quad (9)$$

Such intensities are now available in terawatt tabletop laser systems based on chirped-pulse amplification.<sup>19</sup> In these, a Joule of light is compressed into a picosecond to yield a terawatt of peak power,<sup>‡</sup> which is then focused to a few wavelengths squared, say  $10 \mu\text{m}^2$ , to yield intensity of  $10^{19}$  W/cm<sup>2</sup>. The photon number density at such a focus is about  $10^{27}$ /cm<sup>3</sup>, about 1,000 times the number density of electrons in lead!

Fields approaching the QED critical field strength will occur at the surface of the electron and positron bunch at a future linear collider (as viewed by a particle in the oncoming bunch). If the fields exceed the critical field, the resulting

---

<sup>†</sup>The QED critical field strength was first noted by Sauter<sup>12</sup> as the field strength at which Klein's paradox<sup>13</sup> occurs. Heisenberg and Euler<sup>14</sup> first interpreted it as the field strength at which the vacuum sparks into  $e^+e^-$  pairs. A classical preview of the QED critical field can be gotten from considerations of the radiation reaction.<sup>15</sup>

<sup>‡</sup>A terawatt is the average power consumption of the United States.

disruption of the bunches would limit the luminosity and precision of the center-of-mass energy of the collider.<sup>20</sup>

Thus, there are both basic and applied physics motivations to explore electron-photon interactions near the QED critical field strength.

### 1.3 Multiphoton Effects

If we pursue the QED critical field strength by use of an intense laser beam, we will also encounter another nonlinear electrodynamic effect: interactions in which several laser photons participate simultaneously. This effect has a classical limit: higher multipole radiation.

It is simplest to consider an electron moving inside a circularly polarized laser beam, in the frame in which the electron has no motion along the direction of the laser beam. In general, this is not the lab frame.

We write the laser field strength as  $E$  and its angular frequency as  $\omega_0$ .

The classical response of the electron to the laser beam is transverse motion in a circle with angular velocity  $\omega_0$  and velocity  $v_\perp$  described by

$$\gamma \frac{v_\perp}{c} = \frac{eE}{m\omega_0 c} \equiv \eta. \quad (10)$$

The parameter  $\eta$  is a classical, dimensionless measure of the field strength of a wave, and is Lorentz invariant, as can be seen from the relation

$$\eta = \frac{e\sqrt{\langle A_\mu A^\mu \rangle}}{mc^2}, \quad (11)$$

where  $A_\mu$  is the vector potential and the average is taken over a cycle of the wave.

Thus when  $\eta$  approaches or exceeds unity, the transverse motion of the electron is relativistic inside the wave.

Classically, an accelerating charge radiates, and if the velocity of transverse motion during acceleration is relativistic, the radiation includes higher multipole terms. These are associated with frequencies that are integer multiples of the frequency of the driving wave. The rate of multipole radiation varies as

$$\text{Rate}_n \propto \eta^{2n} \propto I^n, \quad (12)$$

for  $n$ th-order multipole radiation when  $\eta \lesssim 1$ .

In a quantum view,  $n$ th-order multipole radiation corresponds to scattering in which  $n$  photons are absorbed by the electron from the wave before a single

higher-energy photon is emitted. We have given the name “nonlinear Compton scattering” to this multiphoton process.

In our experiment we first explored nonlinear Compton scattering as part of the preparation of the beam of high-energy backscattered photons needed for the study of pair creation.

Along with  $\eta$  we can introduce a second dimensionless measure of the field,  $\Upsilon$ , which is the ratio of the electric field in a suitable frame to the critical field strength. However,  $\Upsilon$  and  $\eta$  are not independent:

$$\Upsilon \equiv \frac{E^*}{E_{\text{crit}}} = \frac{2\gamma E_{\text{lab}}}{E_{\text{crit}}} = \frac{2\gamma\hbar\omega_0}{mc^2}\eta \approx \eta, \quad (13)$$

where the approximation holds for the conditions of our experiment. Thus, we must untangle two different aspects of nonlinear QED: multiphoton effects and critical-field effects.

There is a further subtlety to the behavior of electrons in strong waves. An electron propagating in a (periodic) wave field of strength  $\eta$  can be said to have an effective mass<sup>21</sup>

$$\bar{m} = m\sqrt{1 + \eta^2}. \quad (14)$$

In the classical view, when the transverse oscillations of the electron are relativistic, the electron becomes “heavier.” In a description that emphasizes the longitudinal motion of the electron, the transverse motion can be associated with a “transverse mass” that is added in quadrature with the rest mass to yield the effective mass [Eq. (14)].

In the quantum view, an electron in a strong wave can be described by quasi-particle states (Volkov states<sup>22,23</sup>). An electron with four-momentum  $p_\mu$  in the absence of the field takes on quasimomentum  $q_\mu$  once in a field whose quanta have four-momentum  $k_\mu$ , as given by

$$q_\mu = p_\mu + \frac{\eta^2 m^2}{2k \cdot p} k_\mu, \quad \text{with} \quad q^2 = \bar{m}^2. \quad (15)$$

When discussing energy-momentum conservation for electrons in a wave, one should use quasienergy and quasimomentum, rather than ordinary energy and momentum. The shifted mass of the electron manifests itself in scattering experiments through the resulting changes in, for example, the minimum energy of the scattered electron, or the energy threshold for pair creation.

The Higgs mechanism is another example of the shift of masses of elementary particles due to the presence of a strong background field, albeit one without a classical limit.

One may note in Eq. (15) that if  $k \cdot p$  is small, the quasienergy can be much larger than the ordinary energy, and the electron can be regarded as having been temporarily accelerated longitudinally while inside the wave.<sup>24,25</sup> This condition holds when the laser beam is in the same direction as the motion of the electron (or when the electron is initially at rest). Diffraction of laser beams severely limits the size of the effect in the laboratory. However, this effect may be relevant to the understanding of astrophysical  $\gamma$ -ray production.<sup>24</sup>

## 2 The E-144 Experiment

The program of SLAC experiment E-144 has three aspects thus far:

- measurement of the longitudinal polarization of the electron beam via observation of an asymmetry in Compton scattering,
- observation of nonlinear Compton scattering,

$$e + n\omega_0 \rightarrow e' + \omega, \quad (16)$$

up to fourth order ( $n = 4$ ),

- observation of positrons created in the collision of Compton backscattered photons with a laser beam in the multiphoton Breit-Wheeler reaction,

$$\omega + n\omega_0 \rightarrow e^+ e^-. \quad (17)$$

Experiment E-144 was performed in the Final Focus Test Beam (FFTB<sup>26</sup>) at SLAC with terawatt pulses from a frequency-doubled Nd:glass laser with a repetition rate of 0.5 Hz achieved by a final laser amplifier with slab geometry.<sup>27-30</sup> A schematic diagram of the experiment is shown in Fig. 1. The apparatus was designed to detect electrons that undergo nonlinear Compton scattering, reaction (16), as well as positrons produced in  $e$ -laser interactions by the two-step process of reaction (16) followed by reaction (17).

The laser beam was focused onto the electron beam by an off-axis parabolic mirror of 30-cm focal length with a 17° crossing angle at the interaction point, IP-1, 10 m downstream of the Final Focus.

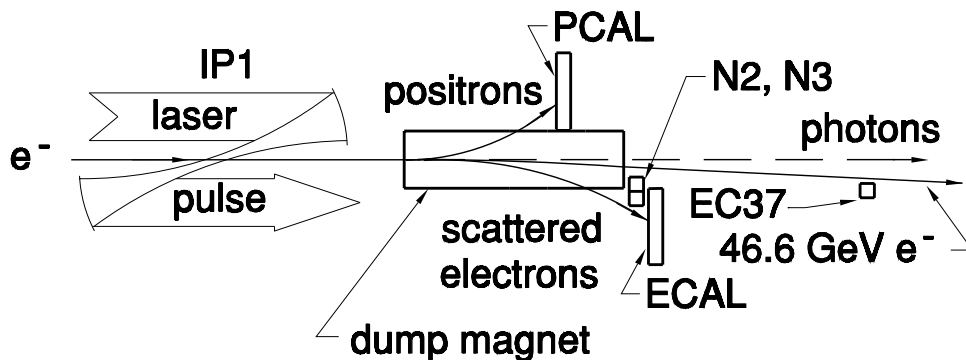


Figure 1: Schematic layout of the experiment.

The laser system is based on the technique of chirped-pulse amplification,<sup>19</sup> as illustrated in Fig. 2. In this technique, a low-energy laser pulse is stretched via a grating pair with the result that the higher frequencies within the pulse propagate earlier than the lower frequencies. In acoustics, such a configuration would sound like a chirp. The stretched pulse is then amplified, and the peak intensities in the amplifier are much less than if the pulse were short. Since damage to the amplifiers is related to peak intensity, greater total energy can be given to a longer pulse. The amplified pulse is still chirped, which permits the pulse to be compressed in time (to a size smaller than the initial width) by a suitably arranged pair of gratings that take out the chirp.

The E-144 laser system is sketched in Fig. 3. It consists of an oscillator, chirping optics, three stages of amplification, pulse-compression optics, and optional frequency-doubling optics. Both linear and circularly polarized beams were available.

The laser-oscillator mode locker was synchronized to the 476-MHz drive of the SLAC linac klystrons with an observed jitter between the laser and linac pulses of 2 ps (rms) (Ref. 29). The scheme of the electron-laser synchronization is shown in Fig. 4.

The peak focused laser intensity was obtained for linearly polarized green (527 nm) pulses of energy  $U = 650$  mJ, focal area  $A \equiv 2\pi\sigma_x\sigma_y = 30 \mu\text{m}^2$ , and width  $\Delta t = 1.6$  ps (fwhm), for which  $I = U/A\Delta t \approx 1.3 \times 10^{18}$  W/cm<sup>2</sup>,  $\eta = 0.36$ , and  $\Upsilon = 0.3$ .

The electron beam was operated at 10–30 Hz with an energy of 46.6 GeV and emittances  $\epsilon_x = 3 \times 10^{-10}$  mrad and  $\epsilon_y = 3 \times 10^{-11}$  mrad. The beam was tuned to



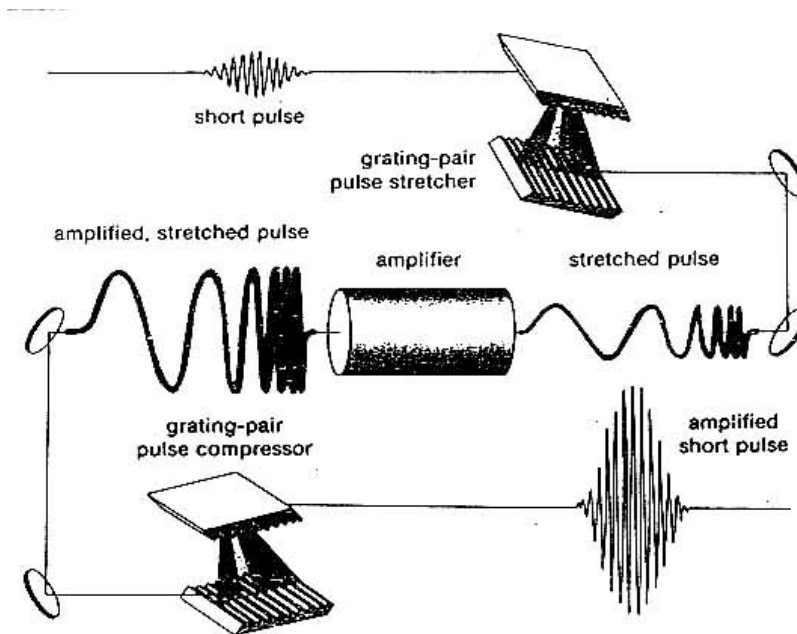


Figure 2: The scheme of chirped-pulse amplification.<sup>19</sup>

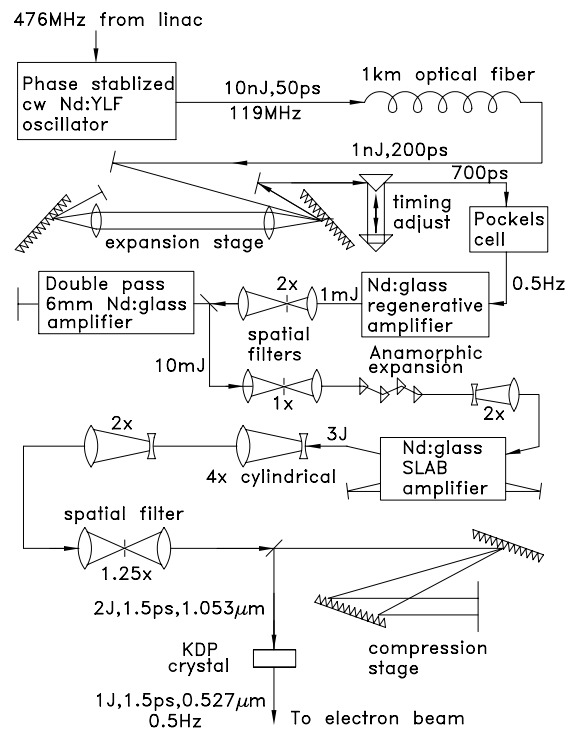


Figure 3: The layout of the E-144 laser system.

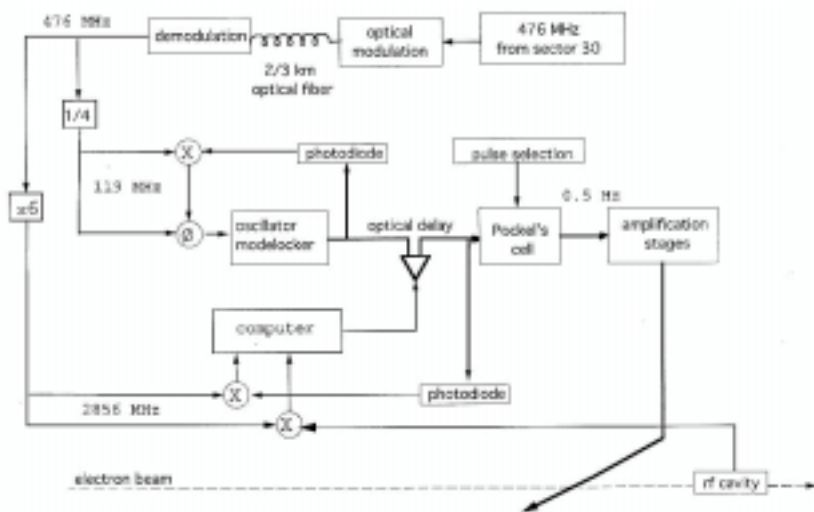


Figure 4: The scheme of electron-laser synchronization.

a focus with  $\sigma_x = 25 \mu\text{m}$  and  $\sigma_y = 40 \mu\text{m}$  at the laser-electron interaction point. Typical bunches were 7 ps long (fwhm) and contained  $7 \times 10^9$  electrons.

A string of permanent magnets after the collision point deflected the electron beam downwards by 20 mrad. Electrons and positrons of momenta less than 20 GeV were deflected by the magnets into two Si-W calorimeters (ECAL and PCAL) as shown in Figs. 1 and 5. The calorimeters were made of alternating layers of silicon ( $300 \mu\text{m}$ ) and tungsten (one radiation length) as illustrated in Fig. 6(a), and measured electromagnetic shower energies with an energy resolution of  $\sigma_E/E \approx 19\%/\sqrt{E[\text{GeV}]}$  and a position resolution of 2 mm. Each layer of silicon was divided into horizontal rows and four vertical columns of  $1.6 \times 1.6 \text{ cm}^2$  active area cells, which allowed the determination of isolated shower positions with a resolution of 2 mm. The Si-W calorimeters were calibrated in parasitic running of the FFTB, in which linac-halo electrons of energies between 5 and 25 GeV were transmitted by the FFTB when the latter was tuned to a lower energy.<sup>31</sup>

Electrons scattered via reaction (16) for  $n = 1, 2,$  and 3 laser photons were measured in gas Cherenkov counters labeled EC37, N2, and N3 in Fig. 1 and shown in more detail in Fig. 6(b). We used detectors based on Cherenkov radiation because of their insensitivity to major sources of low-energy background. EC37 was calibrated by inserting a thin foil in the electron beam at IP-1. The

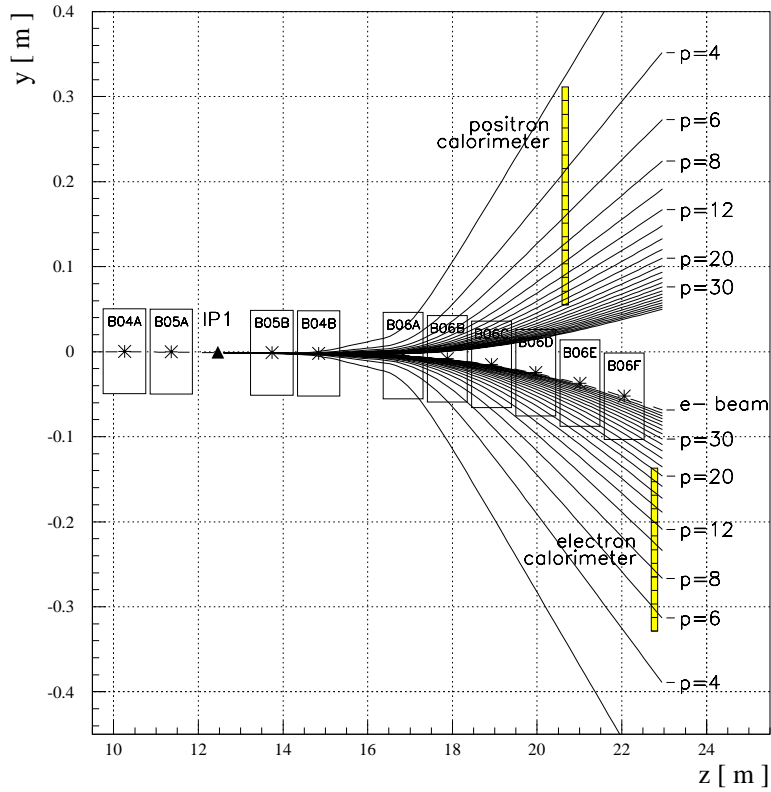


Figure 5: The FFTB dump magnets served as the spectrometer for E-144.

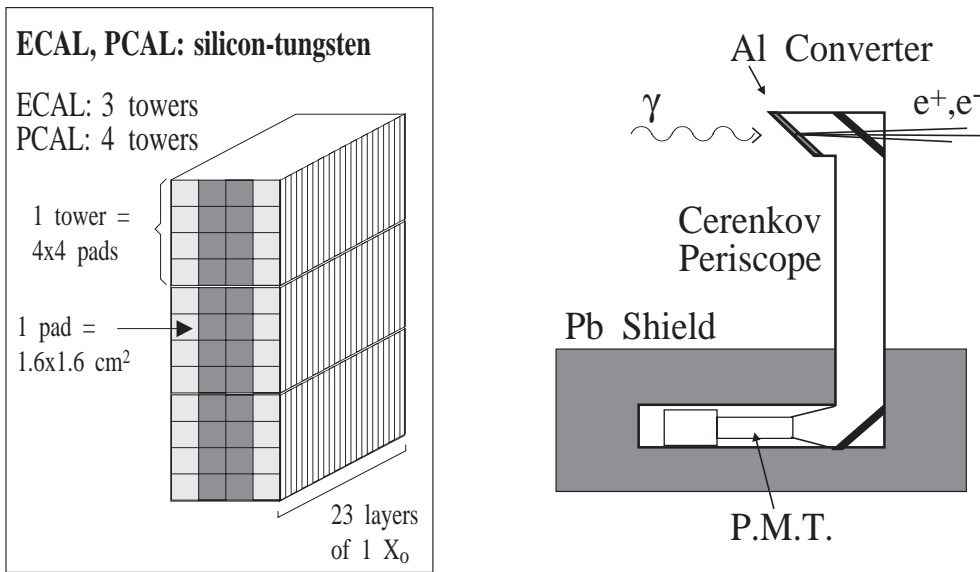


Figure 6: (a) The configuration of the Si-W calorimeters. (b) The Cherenkov monitors of scattered electrons.

momentum acceptance and efficiency of the counters N2 and N3 were measured with the parasitic electron beam by comparison with the previously calibrated ECAL.

The spatial and temporal overlap of the electron and laser beams was optimized by observing the Compton scattering rate of up to  $10^7$ /pulse in the EC37, N2, N3, and ECAL detectors during horizontal, vertical, and time scans of one beam across the other.

### 3 Results

#### 3.1 Electron Polarization

As a first test of the apparatus, we measured the polarization of the electron beam via the dependence of the Compton scattering rate on the longitudinal polarizations of the electron and laser beams.<sup>32</sup> The sign of the polarization of the electron beam varied randomly from pulse to pulse, while the laser beam was set to either left or right circular polarization during runs of a few minutes' duration. The laser pulses were a few mJ in energy at wavelength 527 nm (green) obtained by frequency doubling the infrared pulse.

The observed asymmetries

$$A_L = \frac{N_{L+} - N_{L-}}{N_{L+} + N_{L-}} \quad \text{and} \quad A_R = \frac{N_{R+} - N_{R-}}{N_{R+} + N_{R-}}, \quad (18)$$

where  $L$  and  $R$  refer to left and right circular polarization of the laser and  $+$  and  $-$  refer to the sign of the longitudinal polarization of the electron, are shown in Fig. 7(a). These asymmetries are expected to vanish for scattering at  $90^\circ$  in the center-of-mass frame, which corresponds to 32.0 GeV energy of the electron in the laboratory.

The combined asymmetry,

$$A = \frac{N_{L+} - N_{R+} - N_{L-} + N_{R-}}{N_{L+} + N_{R+} + N_{L-} + N_{R-}}, \quad (19)$$

is shown in Fig. 7(b), which yielded the result

$$P_e P_{\text{laser}} = 0.81 \pm 0.01, \quad (20)$$

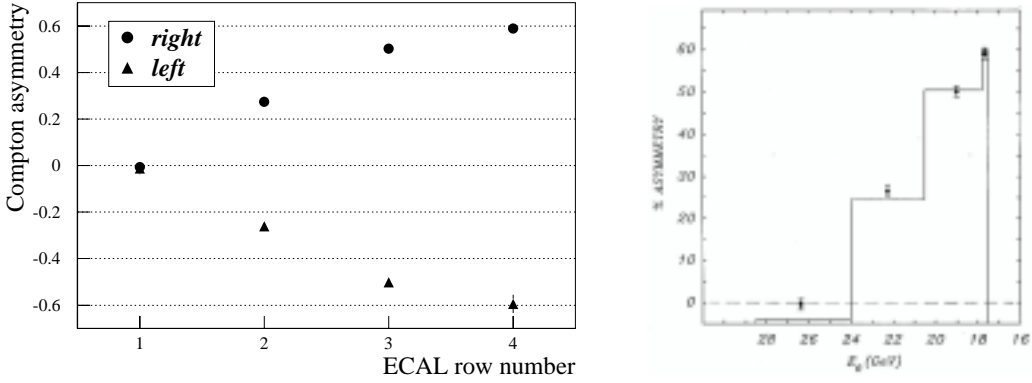


Figure 7: (a) The asymmetries [Eq. (18)] in the Compton scattering rate for left and right circularly polarized laser light as a function of position in the electron calorimeter. (b) The combined asymmetry [Eq. (19)] in the Compton scattering rate as a function of the energy of the scattered electron.

for the product of the polarizations of the two beams. Then, from our separate determination that  $P_{\text{laser}} > 0.96$ , we infer that

$$P_e = 0.81^{+0.04}_{-0.01}, \quad (21)$$

in good agreement with other recent measurements at SLAC.

### 3.2 Nonlinear Compton Scattering

On raising the intensity of the laser pulses, we moved into the regime in which several laser photons could be absorbed by an electron before a single high-energy photon was emitted. This is the process of nonlinear Compton scattering,

$$e + n\omega_0 \rightarrow e' + \omega, \quad (22)$$

in which  $n$  laser photons of frequency  $\omega_0$  participate. This process is indicated schematically in Fig. 8(a). The filled circle at a vertex corresponding to absorption of a laser photon is meant as a reminder that this absorption takes place in a strong background field, and (it turns out) is not characterized by a vertex factor proportional to the charge  $e$ .

The apparatus was configured as in Fig. 9 to study this process. The rate of scattered electrons could be determined as a function of their momentum via their deflection by the FFTB dump magnets into the ECAL calorimeter. The rate of

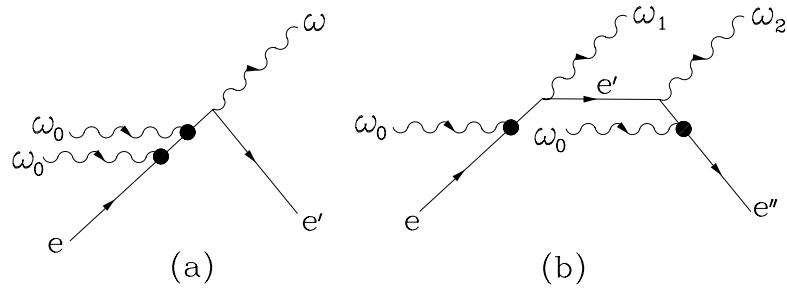


Figure 8: Diagrams for (a) nonlinear Compton scattering, and (b) successive Compton scattering.

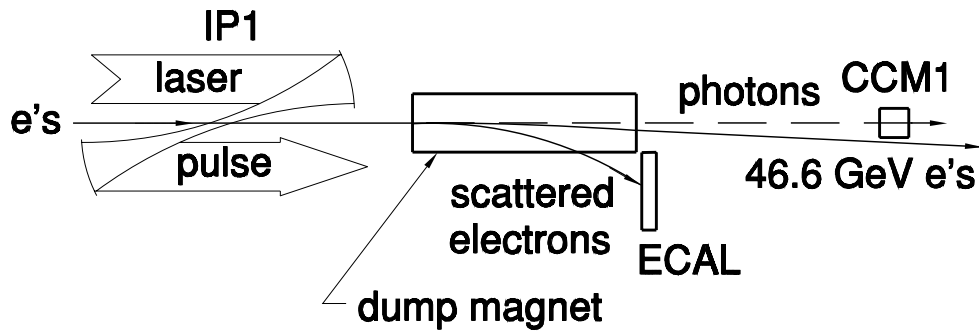


Figure 9: The apparatus for the measurement of nonlinear Compton scattering.

backscattered photons summed over all energies was measured by the Cherenkov monitor CCM1.

Because our analysis is based only on the energy of the scattered electron, we cannot distinguish nonlinear Compton scattering, Eq. (22), from the process of successive Compton scattering, shown in Fig. 8(b). For example, second-order nonlinear Compton scattering leads to the same final energies for the scattered electron as does two first-order Compton scatters in succession. However, successive Compton scattering can be distinguished from nonlinear Compton scattering if the high-energy photon is detected. We report on some measurements of the latter type at the end of this section.

A theoretical calculation of the process of nonlinear Compton scattering has been given by Narozhny, Nikishov, and Ritus,<sup>33,34</sup> among others. The rate for the absorption of  $n$  laser photons by an electron of energy  $E_e$ , leading to final electron energy  $E_{e'}$ , can be written as a sum of Bessel functions,

$$\frac{d\text{Rate}_n}{dE_{e'}} = \frac{4\pi r_0^2 N_{\text{laser}} N_e}{xE_e} \left\{ \left( 2 + \frac{u^2}{1+u} \right) \left[ J_{n-1}^2(z) + J_{n+1}^2(z) - 2J_n^2(z) \right] - \frac{4}{\eta^2} J_n^2(z) \right\}, \quad (23)$$

where

$$x = \frac{4\omega_0 E_e}{m^2}, \quad u \approx \frac{E_e}{E_{e'}} - 1, \quad \text{and} \quad z = \frac{2\eta}{x} \sqrt{nu x - u^2(1 + \eta^2)}, \quad (24)$$

for a circularly polarized laser and unpolarized electrons. The case of a linearly polarized laser is more intricate.

The rate at order  $n$  varies as  $r_0^2 \eta^{2n} \propto \alpha^2 I^n$  for “weak” fields with  $\eta \lesssim 1$ . Nonlinear Compton scattering can be said to be nonperturbative in that the rate does not vary as  $\alpha^{n+1}$ , as might have been expected for a diagram with  $n + 1$  external photons.

The appearance of the Bessel functions in Eq. (23) reminds us that the process of nonlinear Compton scattering has a classical limit that has much in common with synchrotron radiation.<sup>10</sup>

Figure 10(a) shows results of a numerical evaluation of Eq. (23) for parameters typical of E-144, but assuming the laser beam is a monochromatic plane wave. The result expected from the Klein-Nishina formula is shown for comparison as the dashed curve. The electron mass shift raises the minimum electron energy at order  $n = 1$  from 25.4 to 29.3 GeV. The contributions to nonlinear Compton

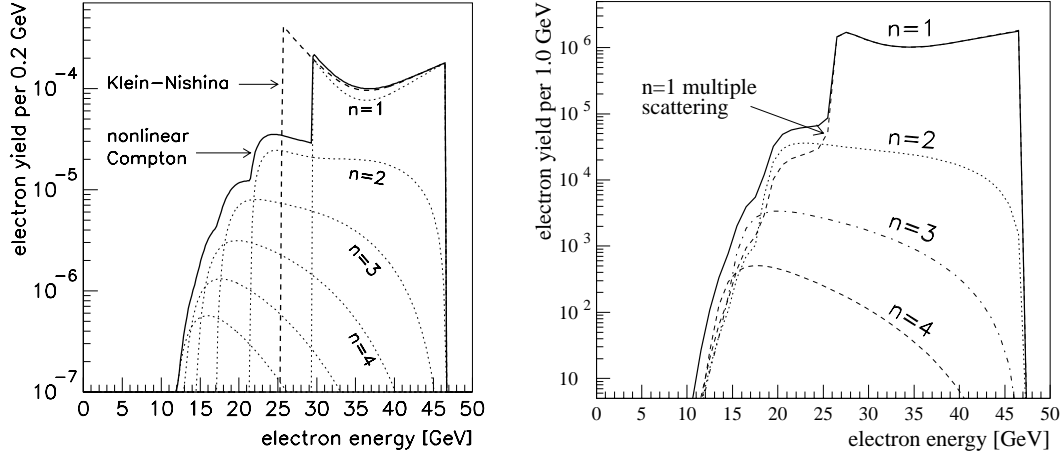


Figure 10: The calculated spectrum of scattered electrons in nonlinear Compton scattering of 46.6-GeV electrons against (a) a 1054-nm plane wave with  $\eta = 0.64$ ; and (b) a 1054-nm laser pulse with  $\eta = 0.64$ , including effects of bunch shape and crossing angle. The yield plotted in (a) is per incident electron; that in (b) is absolute.

scattering at each order are shown in the dotted curves, which sum to the solid curve.

Figure 10(b) shows results of a similar calculation, but taking into account the shapes of the electron and laser pulses, and the  $17^\circ$  crossing angle between the two beams.<sup>35</sup> The effect of the mass shift is much less pronounced now, since there is a large rate at first order in the tails of the laser pulse where  $\eta$  is low. The calculated rate of successive (multiple) Compton scattering is also shown, and is seen to be comparable to that of  $n = 2$  nonlinear Compton scattering, but significantly less than that of higher-order nonlinear Compton scattering.

The observed rates of electrons scattered by circularly polarized laser light at 1054 and 527 nm are shown as a function of laser intensity in Fig. 11.<sup>3,27,31</sup> The rates have been normalized to the  $n = 1$  rate observed in the CCM detector, which renders them less sensitive to fluctuations in the overlap of the electron and laser pulses. The rate at order  $n$  is then expected to vary with intensity as  $I^{n-1}$ . The results of a model calculation are shown as the shaded bands, whose width is a measure of the systematic uncertainty in the laser intensity.

Figure 12 shows representative spectra of scattered electron energy at various intensities of the infrared laser beam. The shaded bands are the results of a model calculation for nonlinear Compton scattering, while the striped bands are for a



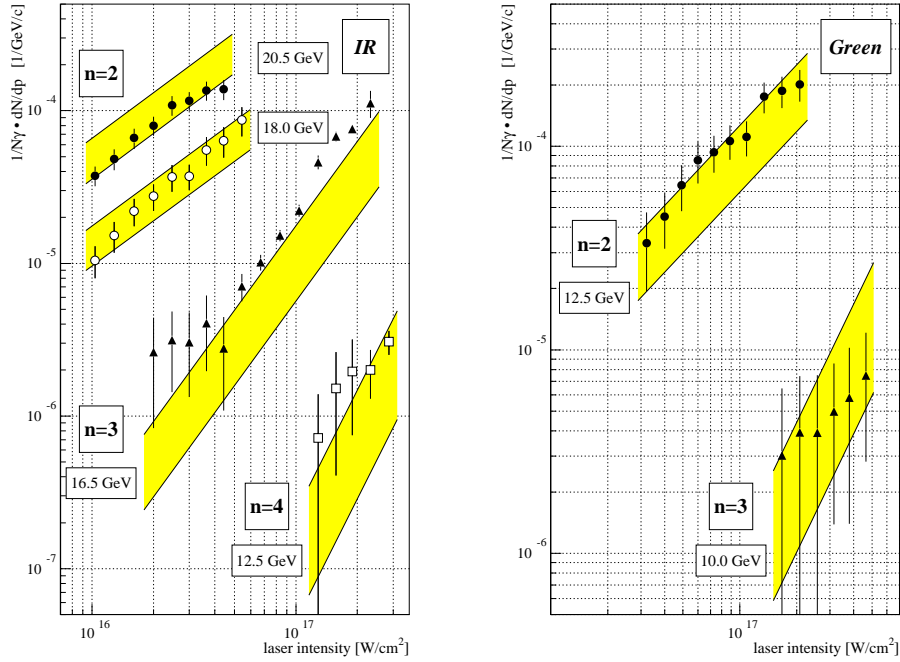


Figure 11: The observed rates of electrons scattered by circularly polarized laser light at 1054 and 527 nm vs laser intensity.

calculation of successive scattering. The kinematic minimum is 17.6 GeV for  $n = 2$  scattering, and 13.5 GeV for  $n = 3$ . The  $n = 2$  edge can be seen in the data, but the  $n = 3$  edge is not resolved. For the highest laser intensities the data are consistent with being almost entirely due to nonlinear Compton scattering rather than successive scattering.

Additional confirmation that we have observed nonlinear Compton scattering was obtained by reconfiguring the apparatus to analyze the spectrum of backscattered photons. The photon calorimeter was replaced by a thin convertor followed by a pair spectrometer, as sketched in Fig. 13. The 5D36 magnet separated the electron and positron from a converted photon by a few centimeters, and the charged particle trajectories were then observed in an array of CCD pixel detectors.

The momentum spectra of the electron and positron have been folded together in Fig. 14(a). The combined spectrum falls steeply to the  $n = 1$  kinematic limit at 29 GeV, above which the  $n = 2$  nonlinear Compton shoulder emerges. That this shoulder is not background can be inferred from Fig. 14(b), in which the ratio of summed rates in the  $n = 1$  and  $n = 2$  regions is plotted as a function of the  $n = 1$

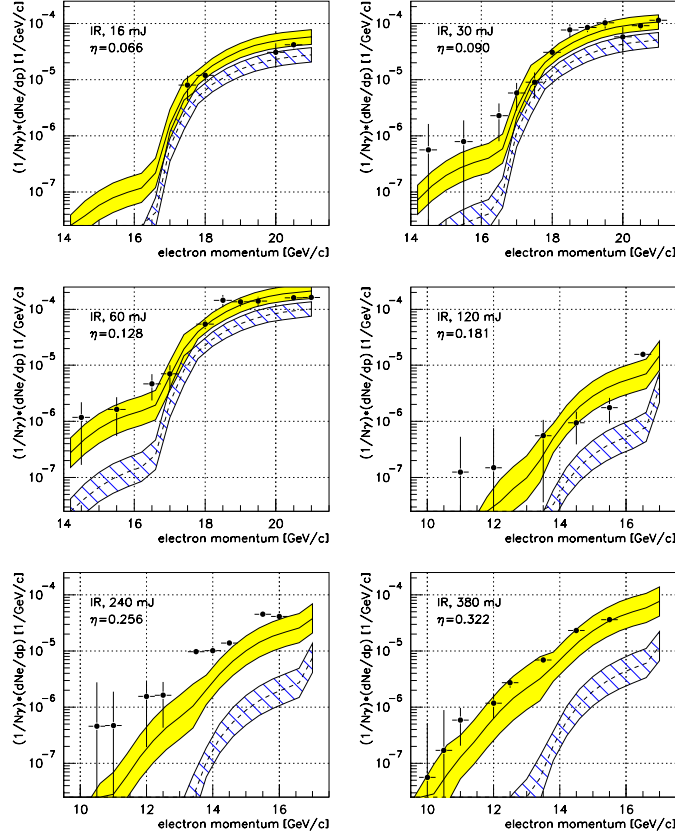


Figure 12: The observed rates of electrons scattered by circularly polarized laser light at 1054 nm vs electron energy for several laser intensities.

rate. The linear rise of the ratio  $N2/N1$  is indicative of the expected quadratic dependence of the  $n = 2$  signal on laser intensity.

### 3.3 Positron Production

Having confidence in our understanding of nonlinear Compton scattering, that is, our understanding of effects that occur as field-strength parameter  $\eta$  approaches one, we then pursued phenomena associated with the approach of parameter  $\Upsilon = E^*/E_{\text{crit}}$  to one, namely effects associated with pair creation in strong fields.

A dramatic effect is the conversion of light into matter via the (multiphoton) reaction

$$\omega + n\omega_0 \rightarrow e^+e^-. \quad (25)$$

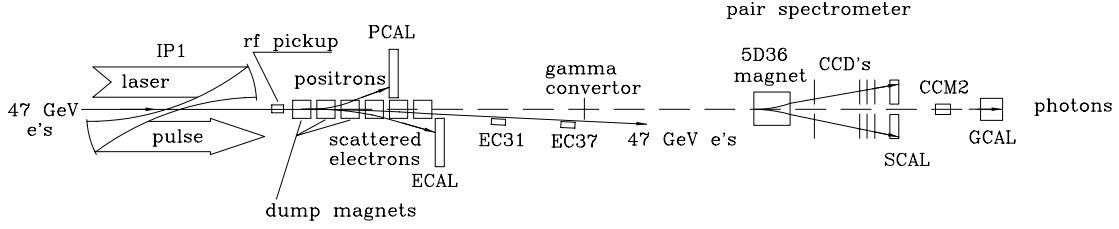


Figure 13: The layout of the apparatus, including the pair spectrometer for analysis of converted, backscattered photons.

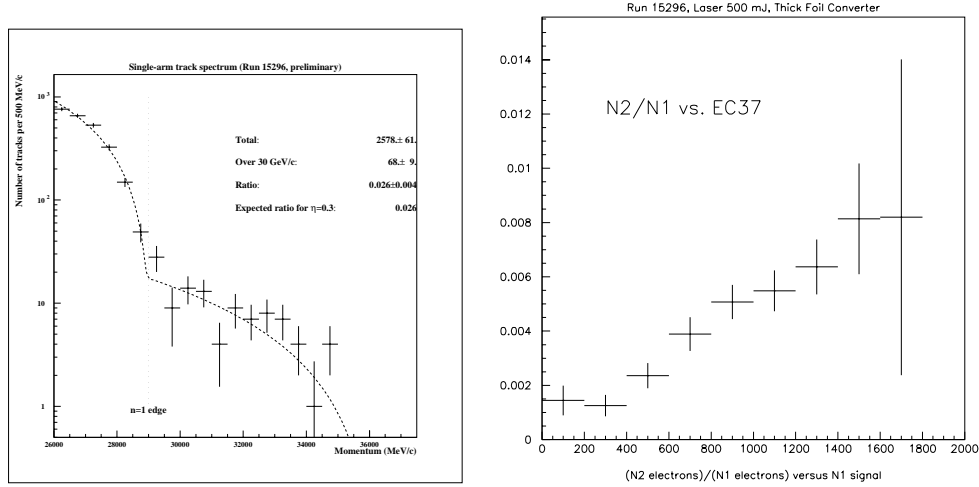


Figure 14: (a) The momentum spectrum of electrons and positrons from conversions of backscattered photons. (b) The ratio of the  $n = 2$  photon rate to the  $n = 1$  photon rate as a function of the latter.

Pair creation via the interaction of two light quanta,

$$\omega + \omega_0 \rightarrow e^+ e^- \quad (26)$$

was first considered in 1934 by Breit and Wheeler,<sup>36</sup> who remarked that although the cross section is of the same order of magnitude as the Compton-scattering cross section, “it is hopeless to try to observe pair formation in laboratory experiments with two beams of  $\gamma$ -rays meeting each other on account of the insufficiently large densities of quanta.” Indeed, this process had not been directly observed prior to the present experiment. It is, however, believed to be responsible for the fall-off of the spectrum of astrophysical  $\gamma$ -rays at very high energies.<sup>37</sup>

The combination of an intense laser beam with the technique of Compton backscattering<sup>38</sup> brings the strong-field reaction (25) within reach of laboratory investigation.

In our experiment, the backscattered photon spectrum extended up to about 30 GeV when we used a 527-nm (2.35-eV photon energy) laser beam to produce the high-energy photons by Compton backscattering, reaction (22). These high-energy photons could then interact with the laser beam before leaving the laser focus to produce pairs via reaction (26). However, the center-of-mass energy of a head-on collision of a 30-GeV photon with a 2.35-eV photon is only 0.52 MeV, which is insufficient to produce pairs. As first noted by Reiss,<sup>39</sup> pair creation can proceed via the multiphoton Breit-Wheeler process (25), the minimum number of laser photons being four in our case.

In the limit of strong fields, the number of laser photons involved becomes large, and it becomes natural to think of the process as pair creation by the strong field rather than by photons. As remarked above in Eq. (13), the parameters  $\eta$  and  $\Upsilon$  are nearly identical in our experiment, so we approach the large- $n$  limit simultaneously with the approach to critical fields.

The multiphoton Breit-Wheeler process, Eq. (25), is the cross-channel process to nonlinear Compton scattering, Eq. (22), and so the theory of the two looks very similar.<sup>33,34,39</sup> Both involve sums of Bessel functions whose argument depends on parameter  $\eta$ . If desired, parameter  $\eta$  could be replaced by the ratio of the laser field strength to the QED critical field (8) calculated in an invariant manner from parameters relevant to reaction (25). Thus, we could introduce the dimensionless ratio  $\Upsilon$  defined by

$$\Upsilon = \frac{\sqrt{\langle (F_{\mu\nu} k^\nu)^2 \rangle}}{mc^2 E_{\text{crit}}}, \quad (27)$$

where  $F_{\mu\nu}$  is the electromagnetic four-tensor of the laser beam and  $k_\mu$  is the four-momentum of the high-energy photon. In particular, when a photon of energy  $\hbar\omega$  collides head-on with a wave of laboratory field strength  $E_{\text{rms}}$  and invariant strength  $\eta$ , we have

$$\Upsilon = \frac{2\hbar\omega E_{\text{rms}}}{mc^2 E_{\text{crit}}} = \frac{2\hbar\omega \lambda_C}{mc^2 \lambda_0} \eta. \quad (28)$$

For example, in a head-on collision of a photon of energy 29 GeV with a 527-nm laser pulse ( $\lambda_0 = 84$  nm),  $\Upsilon = 0.52\eta$ .

The configuration of the apparatus for the study of positron production has already been shown in Fig. 1. As only one electron-positron pair is expected for  $10^9$  Compton scatters during the few picosecond laser pulse, it was not possible to correlate the positrons with their electron partners. We did, however, use signals of

second- and third-order nonlinear Compton scattering in Cherenkov detectors—labeled  $N2$  and  $N3$ —as monitors of the  $e$ -laser interaction, since higher-order processes are more sensitive to the precise overlap of the two beams.

Positrons can also be produced by the interaction of lost beam electrons with material upstream of the positron detector, PCAL, or by conversion of Compton-backscattered photons in residual gas in the beam pipe. By collecting data with the laser off but electron beam on, the first background was determined to be less than one positron per  $10^{12}$  beam electrons—which is a testament to the high quality of the Final Focus Test Beam.

Figure 15(a) shows the number of positron candidates observed in the detector PCAL when running with 46.6-GeV electrons and a 527-nm laser beam, both for the 21,962 laser-on and the 121,216 laser-off pulses.<sup>4</sup> There were 175 laser-on candidates with a background estimated as  $0.175 \cdot 379$  from the laser-off candidates (0.175 being the ratio of the number of laser-on to laser-off pulses). Figure 15(b) shows the subtracted positron spectrum, and compares it to the prediction of a model calculation.<sup>35</sup> The laser-associated positron signal is then  $106 \pm 14$  events.

As will be shown shortly, there is little evidence for positron production in our experiment for values of parameter  $\eta$  below 0.2. Figures 15(c) and (d) show the results of an analysis with the requirement that  $\eta > 0.216$ , which yielded a signal of  $69 \pm 9$  laser-associated positrons. By either analysis the significance of the laser-associated positron signal is seven standard deviations.

Figure 16 shows the yield ( $R_{e+}$ ) of positrons/laser shot as a function of  $\eta$ . The line is a power law fit to the data and gives

$$R_{e+} \propto \eta^{2n} \quad \text{with} \quad n = 5.1 \pm 0.2 \text{ (stat.) }^{+0.5}_{-0.8} \text{ (syst.).} \quad (29)$$

Thus, the observed positron production rate is highly nonlinear, varying as the 5<sup>th</sup> power of the laser intensity. This is in good agreement with the fact that the rate of multiphoton reactions involving  $n$  laser photons is proportional to  $\eta^{2n}$  (for  $\eta^2 \ll 1$ ), and with the kinematic requirement that five photons are needed to produce a pair near threshold [one for the Compton scattering, Eq. (22), and four more for the Breit-Wheeler process, Eq. (25)].

Several points at low values of  $\eta$  seen in Fig. 16, while statistically consistent with Breit-Wheeler pair creation, indicate a possible residual background of about  $2 \times 10^{-3}$  positrons/laser shot due to interactions of Compton backscattered photons with beam gas.

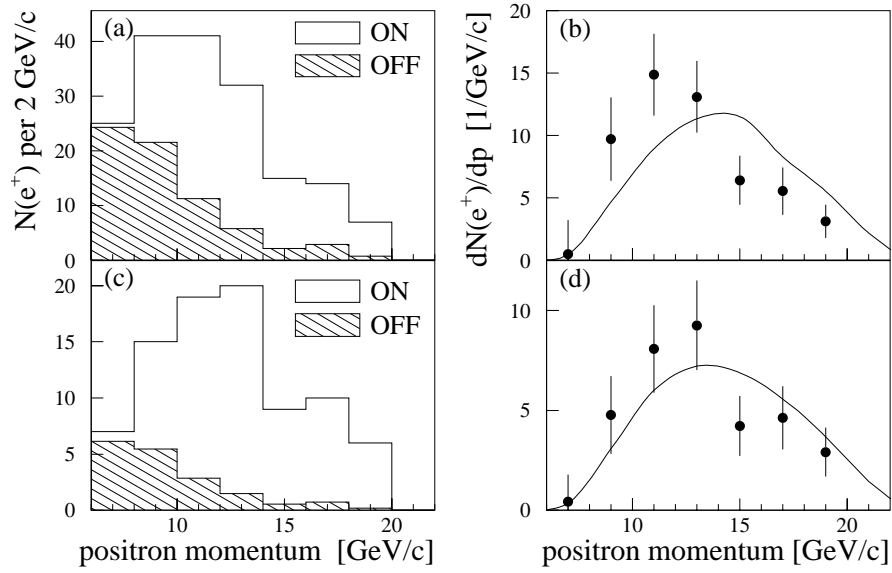


Figure 15: The momentum spectra of positron candidates in laser-on and laser-off pulse, along with the subtracted signal, on—off. No cut on laser intensity is made in (a) and (b), while we required  $\eta > 0.216$  for (c) and (d).

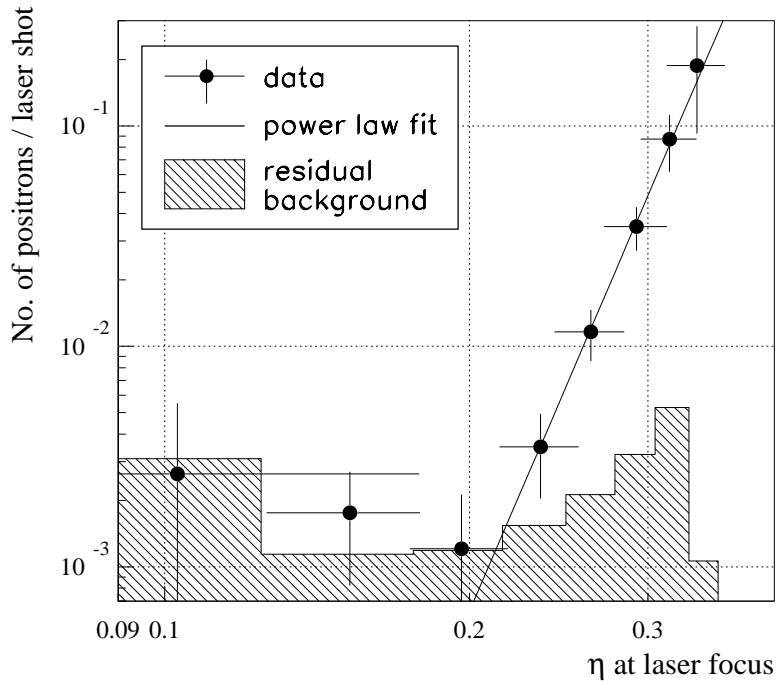


Figure 16: Dependence of the positron rate per laser shot on the laser field-strength parameter  $\eta$ .

The observed positron rate is shown in Fig. 17 after being normalized to the number of Compton scatters, where the latter is inferred from the measured rate in the EC37 Cherenkov monitor. The solid curve in Fig. 17 shows the prediction based on the numerical integration of the two-step Breit-Wheeler process, Eq. (22) followed by Eq. (25) (see Ref. 35). The data are in good agreement with the simulation, both in the magnitude of the observed rate and in its dependence on  $\eta$ .

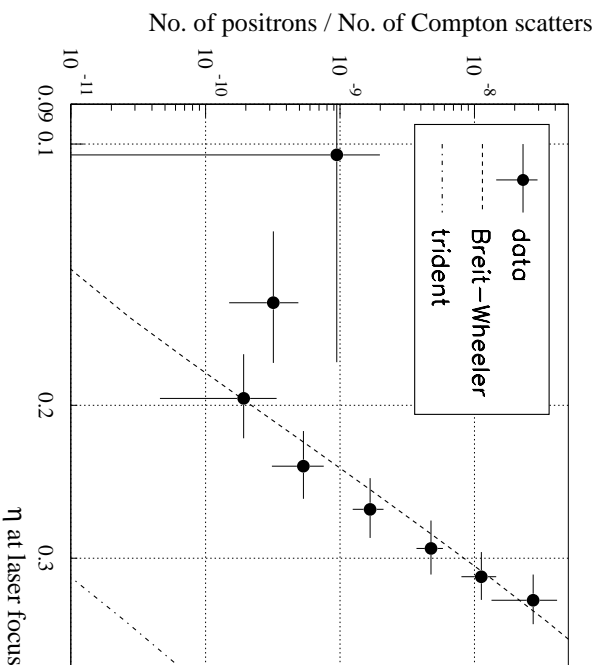


Figure 17: Dependence of the positron rate on the laser field-strength parameter  $\eta$  when the rate is normalized to the number of Compton scatters inferred from the EC37 monitor.

Because we observed positrons emerging from the same interaction point in which the electron and laser beams collide, it is possible that the positrons were created by the (multiphoton) trident process

$$e + n\omega_0 \rightarrow e'e^+e^- . \quad (30)$$

No detailed theory of this process exists in the strong-field regime, so we used a Weizsäcker-Williams approximation in which the beam electron emits a virtual photon which combines with laser photons to yield electron-positron pairs according to the theory of the multiphoton Breit-Wheeler process, Eq. (25) (see Ref. 40). The results of this calculation indicate that for the present experiment the trident process is negligible, as shown in Fig. 17 by the dash-dot line.

It is interesting to compare our results for positron production with the view that the vacuum “sparks” in the presence of a strong field, as first advocated by Euler and Heisenberg.<sup>14</sup> For a virtual  $e^+e^-$  pair to materialize in a field  $E$ , the electron and positron must separate by a distance  $d$  sufficient to extract energy  $2mc^2$  from the field:

$$eEd = 2mc^2. \quad (31)$$

The probability of a separation  $d$  arising as a quantum fluctuation (whose length scale is the Compton wavelength  $\lambda_C$ ) is related to penetration through a barrier of thickness  $d$ :

$$P \propto \exp\left(-\frac{2d}{\lambda_C}\right) = \exp\left(-\frac{4m^2c^3}{e\hbar E}\right) = \exp\left(-\frac{4E_{\text{crit}}}{E}\right) = \exp\left(-\frac{4}{\Upsilon}\right). \quad (32)$$

A more detailed calculation indicates that the factor of four in the numerator of the exponent should actually be  $\pi$  (Refs. 12, 14, and 41).

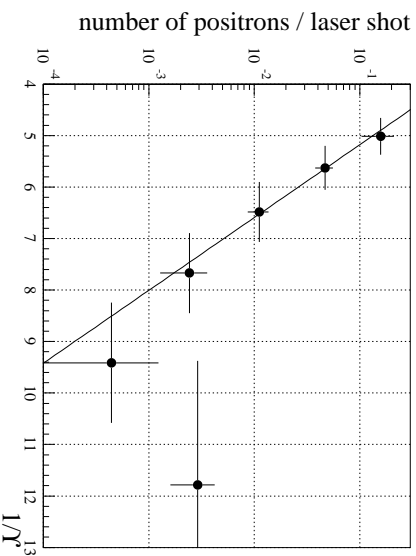


Figure 18: Dependence of the positron rate on  $1/\Upsilon$  as defined by Eq. (27).

To compare Eq. (32) with our data, we use the parameter  $\Upsilon$  as defined in Eq. (27), with results as shown in Fig. 18. A fit yields

$$R_{e^+} \propto \exp[(-2.0 \pm 0.3)/\Upsilon]. \quad (33)$$

The low value of the numerator of the exponent indicates that our laser intensity was not quite high enough for multiphoton pair creation to be in the large- $n$  limit, in which a description based on static fields would suffice.



## 4 Future Directions

### 4.1 Basic Physics

1. Study the mass-shift effect in nonlinear Compton scattering.
  - Continue at SLAC,<sup>2</sup> or use 50-MeV electrons and a CO<sub>2</sub> laser at BNL.<sup>42</sup>
2. Study pair creation in a pure light-by-light scattering situation (see Fig. 19 and Refs. 2 and 11):
  - Could match electron with positron partner.
  - Search for structure in the  $e^+e^-$  invariant-mass spectrum.
  - No trident production.
  - Need upgraded laser: 10-Hz, 100-femtosecond pulses with  $\Upsilon_{\max} \approx 5$ .

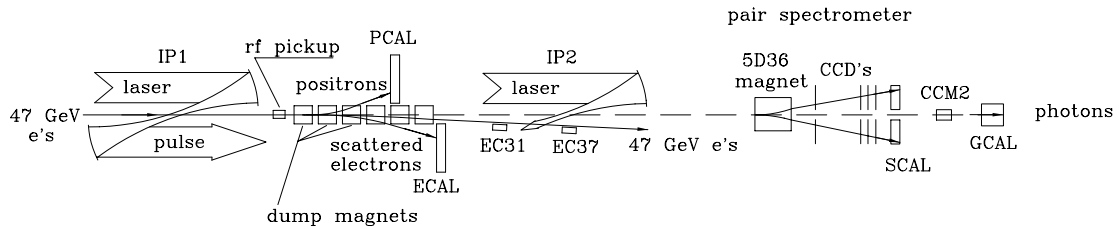


Figure 19: Possible configuration of an experiment to study pair creation at a photon-photon collision point away from the electron beam.

### 4.2 Applied Physics

1. Copious  $e^+e^-$  Production.<sup>43</sup>
  - $e^+e^-$  pairs from  $e$ -laser collisions could be the best low-emittance source of positrons.
  - No Coulomb scattering in laser “target.”
  - Positrons largely preserve the geometric emittance of the electron beam  $\Rightarrow$  “cooling” of invariant emittance.
  - Can produce one positron per electron if  $E^* > E_{\text{crit}}$ .
  - Production with visible laser is optimal for  $\sim 500$  GeV electrons.  
[Or use a 50-nm FEL with 50-GeV electrons.]

2. High-energy  $e\text{-}\gamma$  and  $\gamma\text{-}\gamma$  colliders.<sup>44</sup>
  - $e$ -laser scattering can convert essentially all of an electron beam to a photon beam.
3. Picosecond/femtosecond pulsed- $\gamma$  sources from Compton backscattering.<sup>45</sup>

## Acknowledgments

I acknowledge with pleasure many provocative conversations with Nathan Myhrvold in the 1980s on the topic of strong background fields. John Wheeler has been a constant source of inspiration to pursue the elegant but elusive phenomenon of pair creation by light. Pisin Chen and Bob Palmer have been very helpful in placing the present work in the context of the concerns of contemporary accelerator physics. I have enjoyed discussions of various aspects of strong-field QED with Ian Affleck, Stan Brodsky, Tom Erber, Norman Kroll, Heinz Mitter, Nikolai Narozhny, and Howard Reiss.

Lastly, I wish to acknowledge my E-144 collaborators who did the work summarized here:

- **Princeton University:** Christian Bula, Kathy Canning, Eric Prebys, and Dave Strozzi.
- **University of Rochester:** Charlie Bamber, Todd Blalock, Steve Boege, Uli Haug, Thomas Koffas, Theo Kotseroglou, Adrian Melissinos, Dave Meyerhofer, Dave Reis, and Wolfram Ragg.
- **University of Tennessee:** Steve Berridge, Bill Bugg, Kostya Shmakov, and Achim Weidemann.
- **SLAC:** Dave Burke, Clive Field, Glenn Horton-Smith, Al Odian, Jim Spencer, Dieter Walz, and Mike Woods.

## References

- [1] Many unpublished documents relating to experiment E-144, including those referenced below, can be found at the Internet site <http://www.slac.stanford.edu/exp/e144/notes/notes.html>
- [2] C. Bula *et al.*, "Proposal for a study of QED at critical field strength in intense laser-high energy electron collisions at the Stanford Linear Accelerator Center," E-144 Internal Note (Oct. 20, 1991).
- [3] C. Bula *et al.*, "Observation of nonlinear effects in Compton scattering," *Phys. Rev. Lett.* **76**, 3116 (1996).
- [4] D. L. Burke *et al.*, "Positron production in multiphoton light-by-light scattering," *Phys. Rev. Lett.* **79**, 1626 (1997).
- [5] N. P. Myhrvold, "Vistas in curved space-time quantum field theory," Ph.D. Dissertation, Princeton University (1983).
- [6] S. W. Hawking, "Black hole explosions?" *Nature* **248**, 30 (1974); "Particle creation by black holes," *Comm. Math.-Phys.* **43**, 199 (1975).
- [7] W. G. Unruh, "Notes on black hole evaporation," *Phys. Rev. D* **14**, 870 (1976); "Particle detectors and black hole evaporation," *Ann. N.Y. Acad. Sci.* **302**, 186 (1977).
- [8] J. S. Bell and J. M. Leinaas, "Electrons as accelerated thermometers," *Nuc. Phys. B* **212**, 131 (1983).
- [9] K. T. McDonald, "The Hawking-Unruh temperature and quantum fluctuations in particle accelerators," *Proceedings of the 1987 IEEE Particle Accelerator Conference*, edited by E. R. Lindstrom and L. S. Taylor (Mar. 16–19, 1987, Washington, D.C.), p. 1196.
- [10] K. T. McDonald, "Fundamental physics during violent accelerations," in *Laser Acceleration of Particles*, edited by C. Joshi and T. Katsouleas, *AIP Conference Proceedings No. 130* (New York, 1985), p. 23.
- [11] K. T. McDonald, "Proposal for experimental studies of nonlinear quantum electrodynamics," Princeton U. preprint DOE/ER/3072-38 (Sept. 2, 1986).
- [12] F. Sauter, "Über das Verhalten eines Elektrones im homogenen elektrischen Feld nach der relativistischen Theorie Diracs," *Z. Phys.* **69**, 742 (1931).
- [13] O. Klein, "Reflexion von Elektronen an einem Potentialsprung nach der relativistischen Dynamik von Dirac," *Z. Phys.* **53**, 157 (1929).
- [14] W. Heisenberg and H. Euler, "Folgerungen aus der Diracschen Theorie des Positrons," *Z. Phys.* **98**, 718 (1936).
- [15] K. T. McDonald, "Limitations to the classical concept of the electromagnetic field as inferred from the radiation reaction," (Sept. 11, 1997, submitted to *Am. J. Phys.*).
- [16] See for example, P. A. Sturrock, "A model of pulsars," *Astro. J.* **164**, 529 (1971).
- [17] For reviews see J. S. Greenberg and W. Greiner, "Search for the sparking of the vacuum," *Physics Today* (August 1982), p. 24; W. Greiner *et al.*, "Quantum electrodynamics of strong fields," (Springer-Verlag, Berlin, 1985); but see also G. Taubes, "The one that got away?" *Science* **275**, 148 (1997).
- [18] I. Pomeranchuk, "On the maximum energy which the primary electron of cosmic rays can have on the earth's surface due to radiation in the earth's magnetic field," *J. Phys. (USSR)* **2**, 65 (1940).

- [19] D. Strickland and G. Mourou, *Opt. Comm.* **55**, 447 (1985).
- [20] R. Blankenbecler and S. D. Drell, "Quantum treatment of Beamstrahlung," *Phys. Rev. D* **36**, 277-288 (1987).
- [21] T. W. B. Kibble, "Frequency shift in high-intensity Compton scattering," *Phys. Rev.* **138**, B740 (1965); "Radiative corrections to Thomson scattering from laser beams," *Phys. Lett.* **20**, 627 (1966); "Refraction of electron beams by intense electromagnetic waves," *Phys. Rev. Lett.* **16**, 1054 (1966); "Mutual refraction of electrons and photons," *Phys. Rev.* **150**, 1060 (1966); "Some applications of coherent states," "Cargèse lectures in physics," Vol. 2, edited by M. Lévy (Gordon and Breach, New York, 1968), p. 299.
- [22] D. M. Volkov, "Über eine Klasse von Lösungen der Diracschen Gleichung," *Z. Phys.* **94**, 250 (1935).
- [23] See also Secs. 40 and 101 of V. R. Berestetskii, E. M. Lifshitz, and L. P. Pitaevskii, *Quantum Electrodynamics*, 2nd ed. (Pergamon Press, Oxford, 1982).
- [24] K. T. McDonald and K. Shmakov, "Temporary acceleration of electrons while inside an intense electromagnetic pulse," E-144 Internal Note (Sept. 23, 1997).
- [25] K. T. McDonald, "A relativistic electron can't extract net energy from a free wave," E-144 Internal Note (Aug. 22, 1997).
- [26] V. Balakin *et al.*, "Focusing of submicron beams for TeV-scale  $e^+e^-$  linear colliders," *Phys. Rev. Lett.* **74**, 2479 (1995).
- [27] T. Kotseroglou, "Observation of nonlinear Compton scattering," Ph.D. thesis, Univ. of Rochester, UR-1459 (Jan. 1996).
- [28] S. J. Boege, "Evidence of light-by-light scattering with real photons," Ph.D. thesis, Univ. of Rochester, UR-1458 (Jan. 1996).
- [29] T. Kotseroglou *et al.*, "Picosecond timing of terawatt laser pulses with the SLAC 46 GeV electron beam," *Nucl. Instrum. Methods A* **383**, 309 (1996).
- [30] C. Bamber *et al.*, "0.5 Hz, phase-stabilized terawatt laser system with a Nd:glass slab amplifier for nonlinear QED experiments," *Laser Physics* **7**, 135 (1997).
- [31] K. D. Shmakov, "Study of nonlinear QED effects in interactions of terawatt laser with high energy electron beam," Ph.D. thesis (Univ. of Tennessee, Aug. 1997).
- [32] M. S. Woods *et al.*, "Measurement of the longitudinal polarization of the final focus test beam," E-144 Internal Note (Oct. 17, 1994).
- [33] A. I. Nikishov and V. I. Ritus, "Quantum processes in the field of a plane electromagnetic wave and in a constant field I," *Sov. Phys. JETP* **19**, 529, 1191 (1964); "Quantum processes in the field of a plane electromagnetic wave and in a constant field II," **19**, 1191 (1964); "Nonlinear effects in Compton scattering and pair production owing to absorption of several photons," **20**, 757 (1965); "Pair production by a photon and photon emission by an electron in the field of an intense electromagnetic wave and in a constant field," **25**, 1135 (1967).
- [34] N. B. Narozhny *et al.*, "Quantum processes in the field of a circularly polarized electromagnetic wave," *Sov. Phys. JETP* **20**, 622 (1965).
- [35] C. Bula, "A numeric integration program to simulate nonlinear QED processes in electron-laser or photon-laser collisions," E-144 Internal Note (June 12, 1997).
- [36] G. Breit and J. A. Wheeler, "Collision of two light quanta," *Phys. Rev.* **46**, 1087 (1934).

- [37] O. C. De Jager *et al.*, “Estimate of the intergalactic infrared radiation field from  $\gamma$ -ray observations of the galaxy Mrk421,” *Nature* **369**, 294 (1994).
- [38] R. H. Milburn, “Electron scattering by an intense polarized photon field,” *Phys. Rev. Lett.* **10**, 75 (1963).
- [39] H. R. Reiss, “Absorption of light by light,” *J. Math. Phys.* **3**, 59 (1962). “Production of electron pairs from a zero-mass state,” *Phys. Rev. Lett.* **26**, 1072 (1971).
- [40] C. Bula and K. T. McDonald, “The Weizsäcker-Williams approximation to trident production in electron-photon collisions,” E-144 Internal Note (Feb. 28, 1997).
- [41] J. Schwinger, “On gauge invariance and vacuum polarization,” *Phys. Rev.* **82**, 664 (1951).
- [42] R. C. Fernow *et al.*, “Proposal for an experimental study of nonlinear Compton scattering,” submitted to the BNL Center for Accelerator Physics (Oct. 27, 1989).
- [43] P. Chen and R. B. Palmer, “Coherent pair creation as a positron source for a linear collider,” in *Advanced Accelerator Concepts*, edited by J. S. Wurtele, *AIP Conference Proceedings* **279**, 888 (1993).
- [44] “Zeroth order design report for the Next Linear Collider,” SLAC-R-0474-VOL-1 (May 1996), Appendix B.
- [45] R. W. Schoenlein *et al.*, “Femtosecond x-ray pulses at 0.4 Å generated by 90° Thomson scattering,” *Science* **274**, 236 (Oct. 11, 1996).